

Modeling Intrinsic Detection Latency and Timing Jitter in SNSPDs

J. P. Allmaras^{1,4,*}, B. A. Korzh¹, Q-Y. Zhao³, S. Frasca¹, E. Ramirez¹, E. Bersin^{1,3}, M. Colangelo³, D. Zhu³, A. E. Dane³, E. E. Wollman¹, F. Marsili¹, M. D. Shaw¹, K. K. Berggren³ and A. G. Kozorezov²

1. Jet Propulsion Laboratory, California Institute of Technology, Pasadena, CA, USA

2. Department of Physics, Lancaster University, Lancaster, UK

3. Massachusetts Institute of Technology, Cambridge, MA, USA

4. Applied Physics, California Institute of Technology, Pasadena, CA, USA

* jallmara@caltech.edu

Toward Semi-Quantitative Modeling of SNPSD Physics

- Why bother?
 - Optimized device design requires the ability to predict response in different geometries, bias conditions, photon energies
- Metrics for Comparison:
 - PCR curves: energy dependence, shape
 - Intrinsic Jitter: energy and bias dependence
 - Relative Latency: energy and bias dependence

Toward Semi-Quantitative Modeling of SNPSD Physics

- Why bother?
 - Optimized device design requires the ability to predict response in different geometries, bias conditions, photon energies
- Metrics for Comparison:
 - PCR curves: energy dependence, shape
 - **Intrinsic Jitter**: energy and bias dependence
 - **Relative Latency**: energy and bias dependence

Model: TDGL + Electrothermal Equations

2 Temperature Electrothermal Equations

$$\frac{\partial}{\partial t} \left(\frac{\pi^2 k_B^2 N(0) T_e^2}{3} - E_0 \mathcal{E}_s(T_e, |\Delta|) \right) = \nabla \kappa_s(T_e, |\Delta|) \nabla T_e - \frac{96 \zeta(5) N(0) k_B^2}{\tau_0} \frac{T_e^5 - T_{ph}^5}{T_c^3} + \vec{j} \vec{E}$$

$$\frac{\partial T_{ph}^4}{\partial t} = - \frac{T_{ph}^4 - T_{sub}^4}{\tau_{esc}} + \gamma \frac{24 \zeta(5)}{\tau_0} \frac{15}{\pi^4} \frac{T_e^5 - T_{ph}^5}{T_c}$$

Modified Time-Dependent Ginzburg-Landau Equations (TDGL)

$$\frac{\pi \hbar}{8 k_B T_c} \left(\frac{\partial}{\partial t} + \frac{2ie\varphi}{\hbar} \right) \Delta = \xi_{mod}(T_e)^2 \left(\nabla - \frac{2ie}{\hbar c} A \right)^2 \Delta + \left(1 - \frac{T_e}{T_c} - \frac{|\Delta|^2}{\Delta_{mod}(T_e)^2} \right) \Delta + i \frac{\text{div } \vec{j}_s^{Us} - \text{div } \vec{j}_s^{GL}}{|\Delta|} \frac{\hbar D}{\sigma_n \sqrt{2} \sqrt{1 + T_e/T_c}}$$

$$-\sigma_n \nabla^2 \varphi = -\text{div } \vec{j}_s^{Us} \quad \text{Current Conservation}$$

- Solves the time evolution of Order Parameter (Δ), Electric Potential (φ), Temperatures (T_e , T_{ph})

Model Predictions

- Qualitatively consistent with previous literature
 - Detection energy shifts from 'Bell' to 'W' as bias current decreases

- Parameters:

$$W = 100 \text{ nm}$$

$$T_c = 8.65 \text{ K}$$

$$d = 7 \text{ nm}$$

$$\rho_{sq} = 587.5 \Omega_{sq}$$

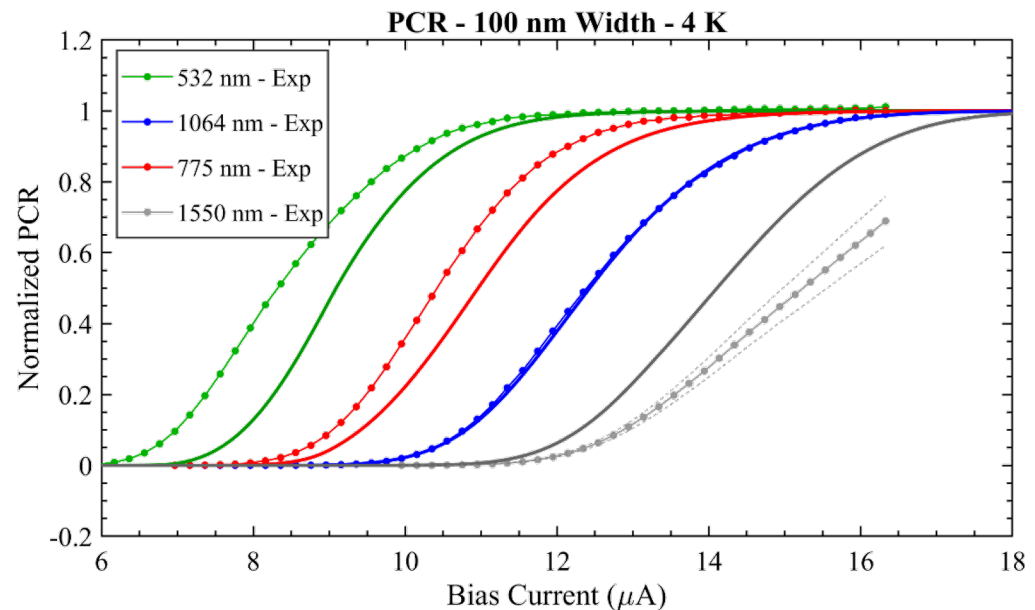
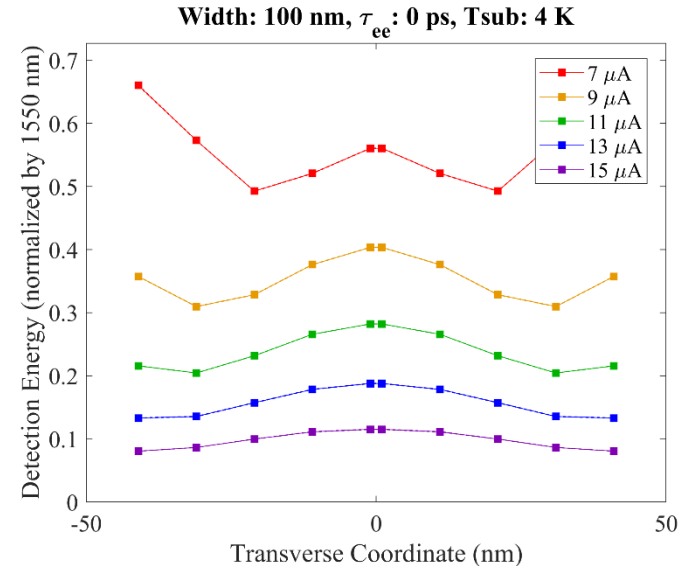
$$T_{sub} = 4 \text{ K}$$

$$\tau_{ep}(T_c) = 16 \text{ ps} (10\text{K}/8.65\text{K})^3 = 24.7 \text{ ps}$$

$$\tau_{esc} = 25 \text{ ps}$$

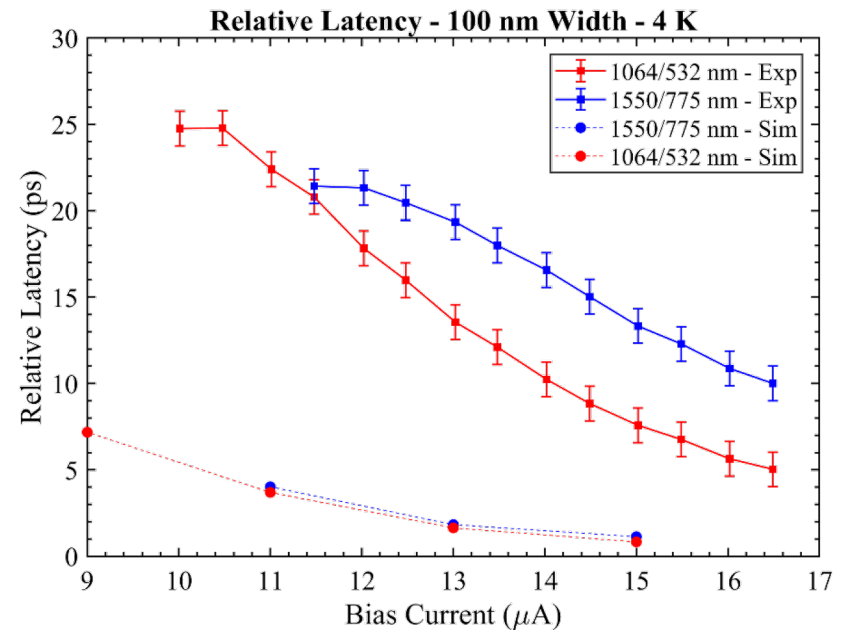
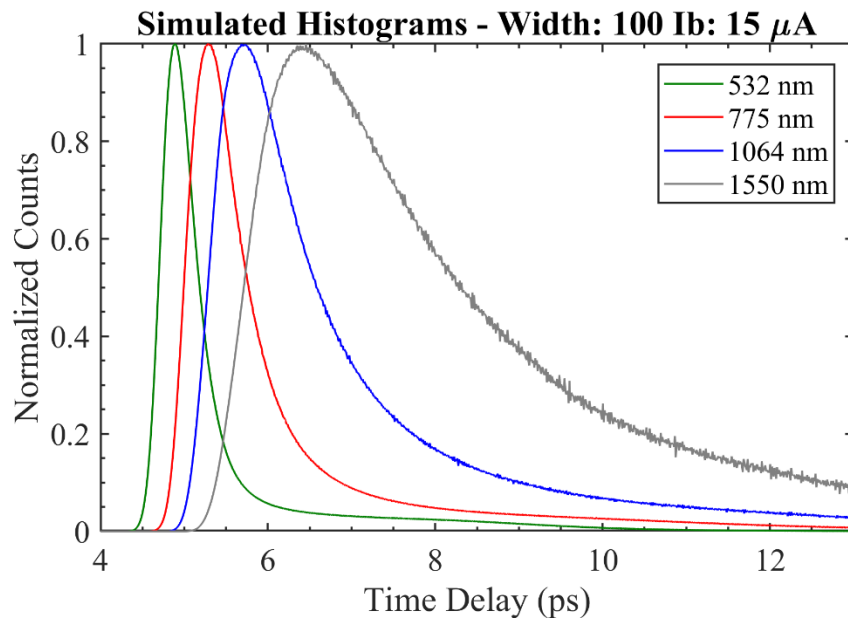
$$D = 0.5 \text{ cm}^2/\text{s}$$

$$I_{dep}(0) \sim 33.4 \mu\text{A}$$



Importance of Detection Latency

- Formulation using standard TDGL equations predicts latency difference much shorter than observed experimentally



Generalized TDGL Equations

- Extends the standard TDGL equations to allow for finite energy gap
 - Includes scattering parameter which modifies the rate of order parameter evolution

$$\frac{\pi \hbar}{8k_B T_c} \left(\varrho(T_e) \frac{\partial}{\partial t} |\Delta| + \frac{i|\Delta|}{\varrho(T_e)} \frac{\partial}{\partial t} \phi + \frac{2ie|\Delta|}{\varrho(T_e)\hbar} \varphi \right) = \xi_{mod}(T_e)^2 \left(\nabla + i \left(\nabla \phi - \frac{2e}{\hbar c} A \right) \right)^2 |\Delta| + \left(1 - \frac{T_e}{T_c} - \frac{|\Delta|^2}{\Delta_{mod}^2(T_e)} \right) |\Delta|$$

$$+ i \frac{(\nabla \cdot \vec{j}_s^{Us} - \nabla \cdot \vec{j}_s^{GL})}{|\Delta|} \frac{\hbar e D}{\sigma_n \sqrt{2} \sqrt{1 + T_e/T_c}}$$

$$\varrho(T_e) = \sqrt{1 + |\Delta|^2 \tau_{sc}(T_e)^2 / \hbar^2} \left. \vphantom{\varrho(T_e)} \right\} \begin{array}{l} \text{Time} \\ \text{evolution} \\ \text{scale factor} \end{array}$$

Inelastic scattering time

- We retain the modifying terms added by Vodolazov (2017)

Watts-Tobin et al., *J. Low Temp. Phys.* **42**, 459 (1981)

Kopnin, *Theory of Nonequilibrium Superconductivity* (2001)

Generalized TDGL Equations

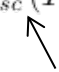
- Extends the standard TDGL equations to allow for finite energy gap
 - Includes scattering parameter which modifies the rate of order parameter evolution

$$\frac{\pi\hbar}{8k_B T_c} \left(\varrho(T_e) \frac{\partial}{\partial t} |\Delta| + \frac{i|\Delta|}{\varrho(T_e)} \frac{\partial}{\partial t} \phi + \frac{2ie|\Delta|}{\varrho(T_e)\hbar} \varphi \right) = \xi_{mod}(T_e)^2 \left(\nabla + i \left(\nabla \phi - \frac{2e}{\hbar c} A \right) \right)^2 |\Delta| + \left(1 - \frac{T_e}{T_c} - \frac{|\Delta|^2}{\Delta_{mod}^2(T_e)} \right) |\Delta|$$

$$+ i \frac{(\nabla \cdot \vec{j}_s^{Us} - \nabla \cdot \vec{j}_s^{GL})}{|\Delta|} \frac{\hbar e D}{\sigma_n \sqrt{2} \sqrt{1 + T_e/T_c}}$$

$\varrho(T_e) = \sqrt{1 + |\Delta|^2 \tau_{sc}(T_e)^2 / \hbar^2}$

$\left. \vphantom{\varrho(T_e)} \right\}$ Time evolution scale factor


 Inelastic scattering time

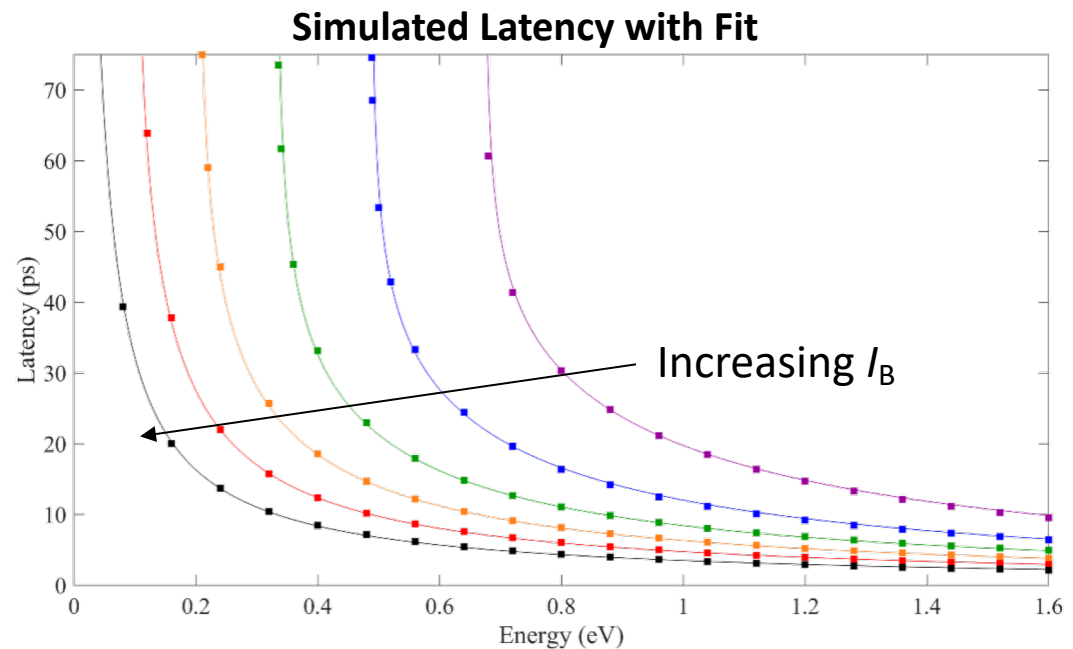
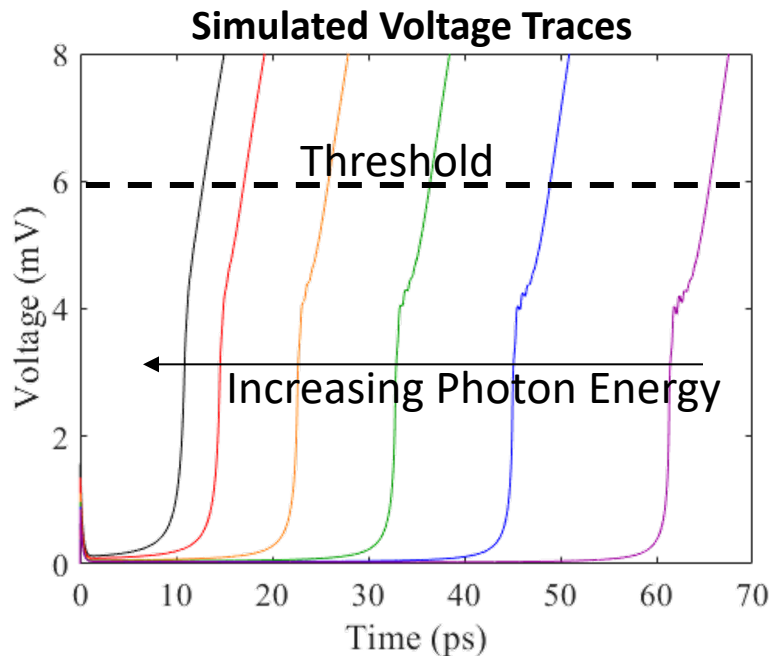
- We retain the modifying terms added by Vodolazov (2017)

Watts-Tobin et al., *J. Low Temp. Phys.* **42**, 459 (1981)

Kopnin, *Theory of Nonequilibrium Superconductivity* (2001)

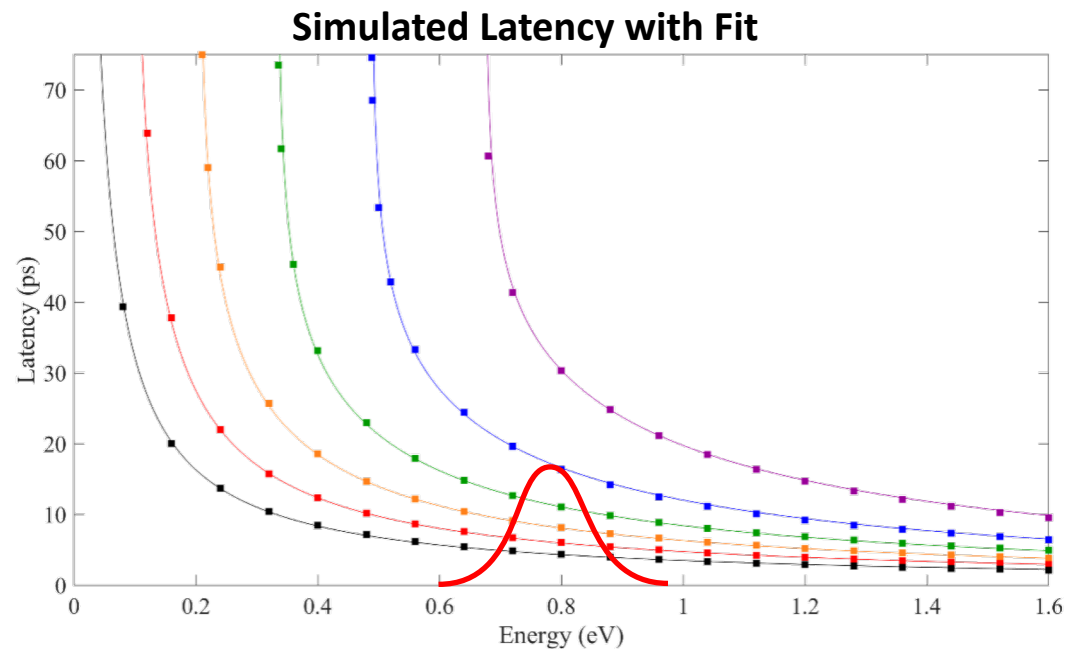
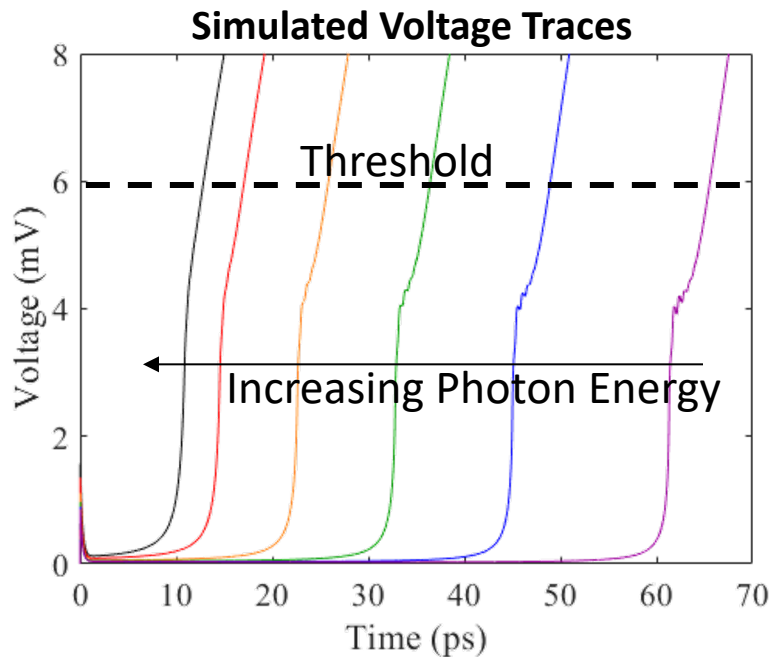
1-Dimensional Model

- Neglects 2D effects in favor of understanding the timescale of order parameter suppression during detection
- ‘Hotbelt’ initial conditions
- Deterministic evolution based on initial conditions
- Jitter caused by Fano fluctuations



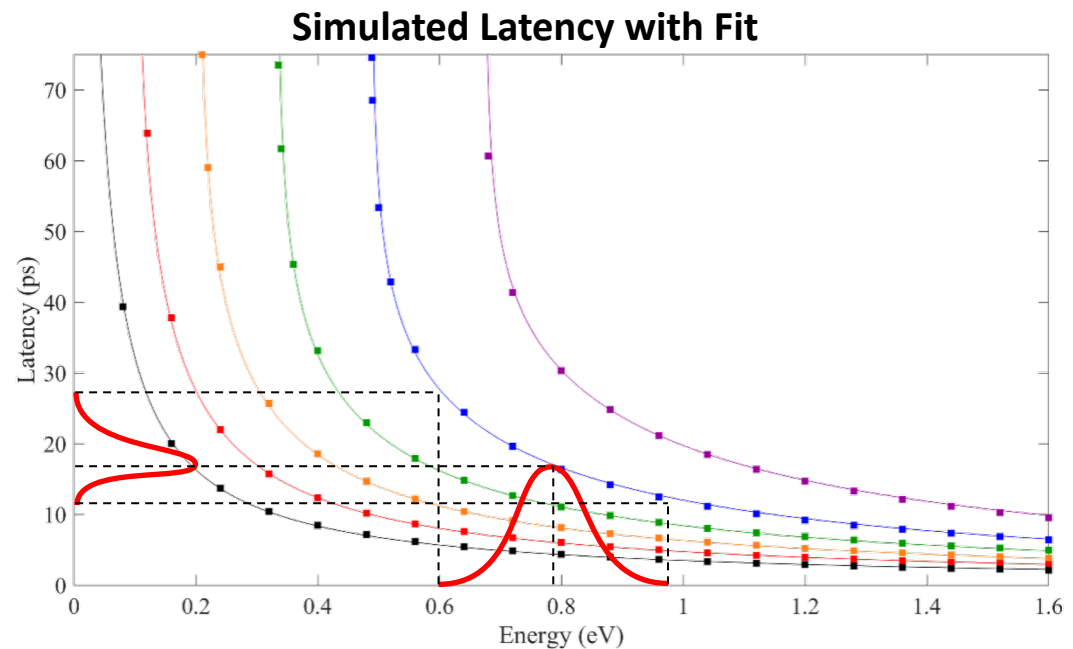
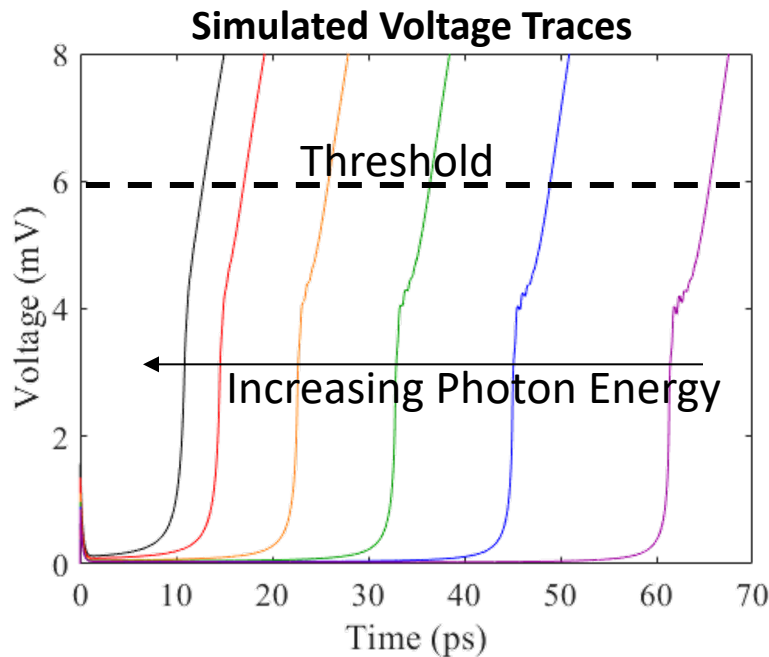
1-Dimensional Model

- Neglects 2D effects in favor of understanding the timescale of order parameter suppression during detection
- ‘Hotbelt’ initial conditions
- Deterministic evolution based on initial conditions
- Jitter caused by Fano fluctuations



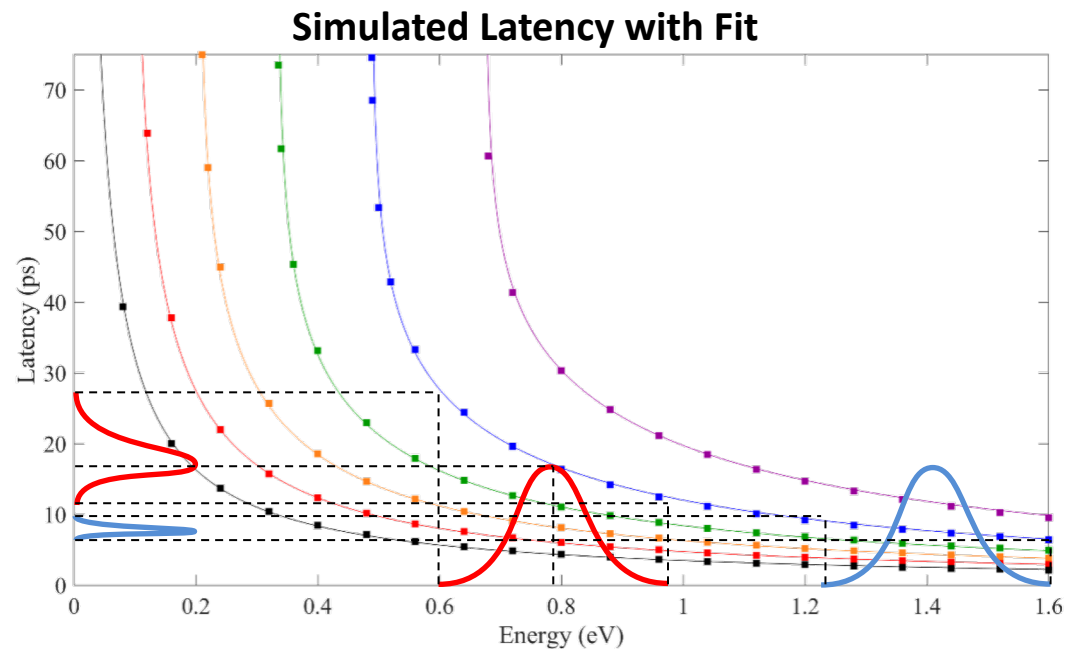
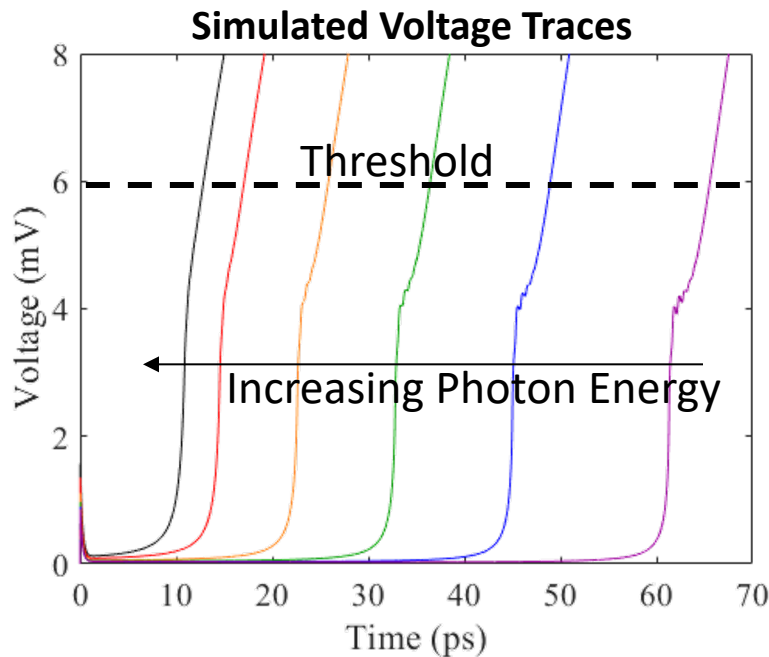
1-Dimensional Model

- Neglects 2D effects in favor of understanding the timescale of order parameter suppression during detection
- ‘Hotbelt’ initial conditions
- Deterministic evolution based on initial conditions
- Jitter caused by Fano fluctuations



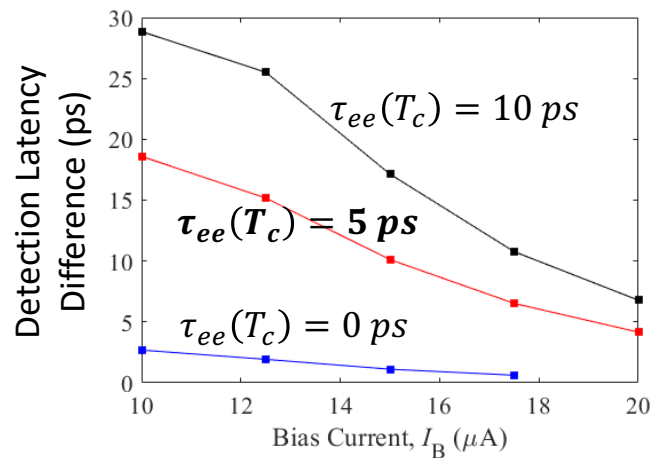
1-Dimensional Model

- Neglects 2D effects in favor of understanding the timescale of order parameter suppression during detection
- ‘Hotbelt’ initial conditions
- Deterministic evolution based on initial conditions
- Jitter caused by Fano fluctuations

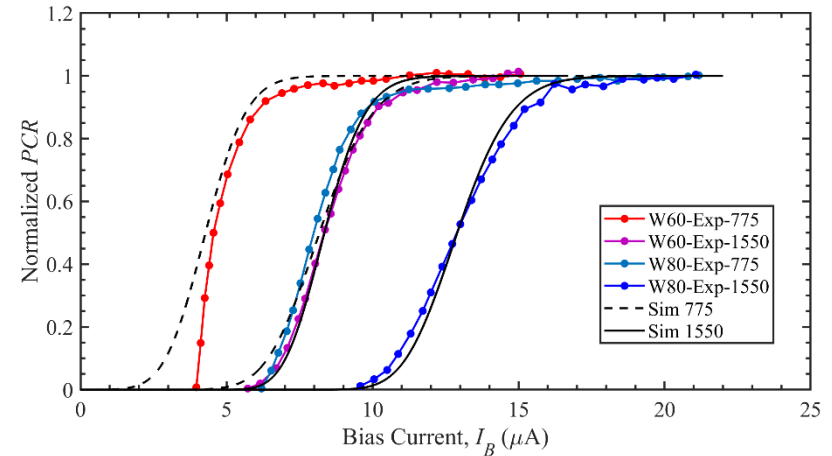


1-Dimensional Model

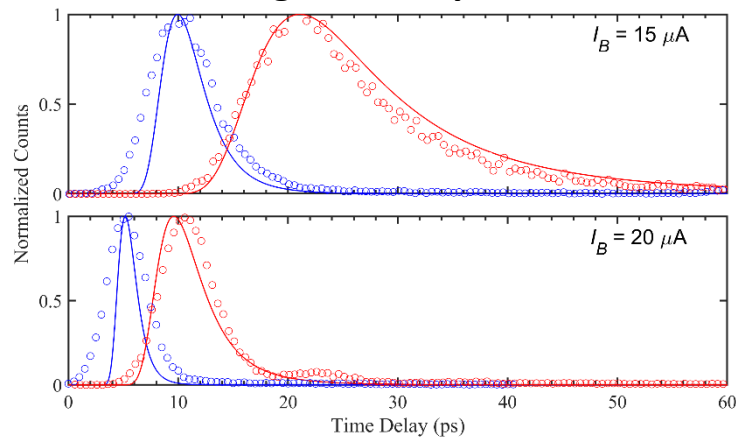
Latency Comparison – Scattering Time



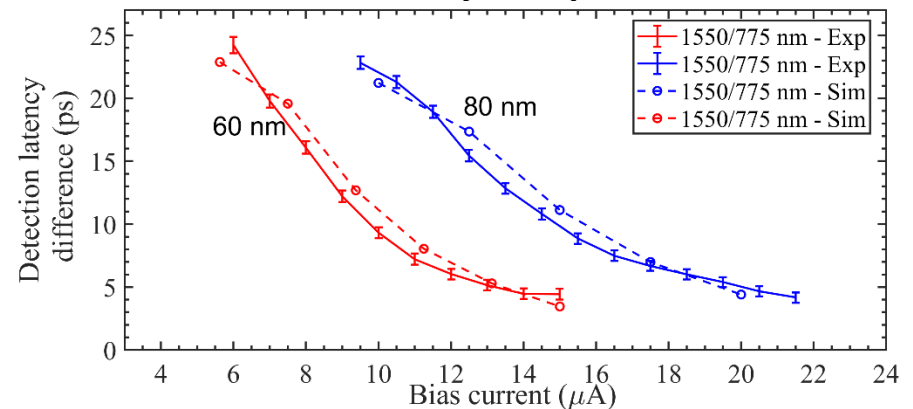
PCR Comparison



Histogram Comparison



Latency Comparison



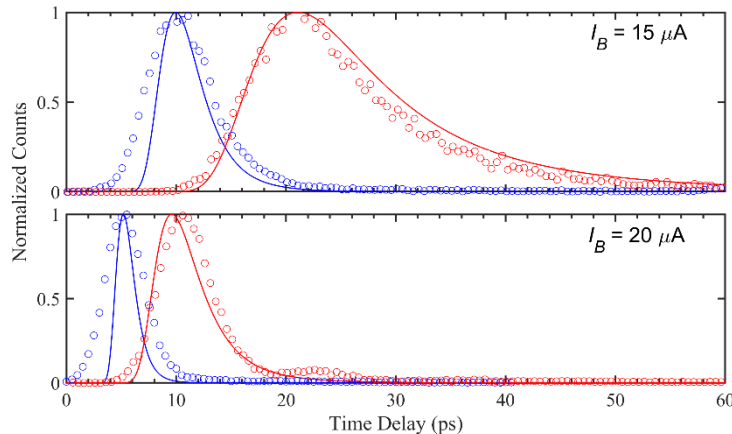
1-Dimensional Model

Latency Comparison – Scattering Time

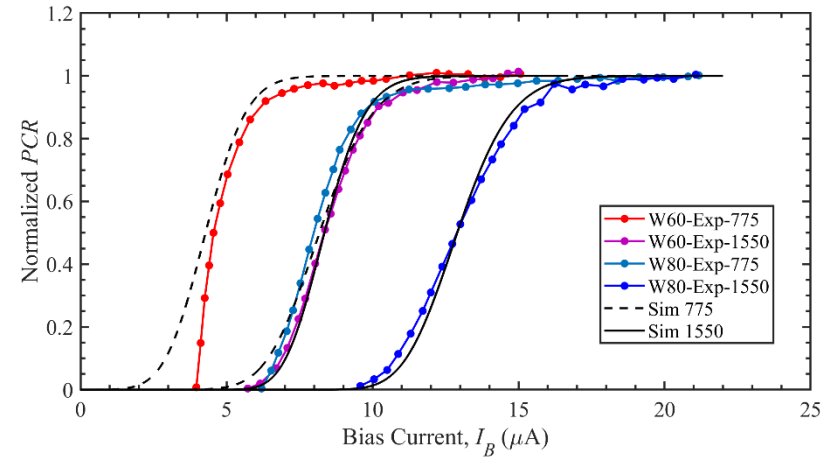
- Introduction of latency + Fano fluctuations qualitatively describes all observed behavior in narrow devices
- 1D model fails over a more extended range of photon energies
- 1D model fails for wider nanowires

Bias Current, I_B (μA)

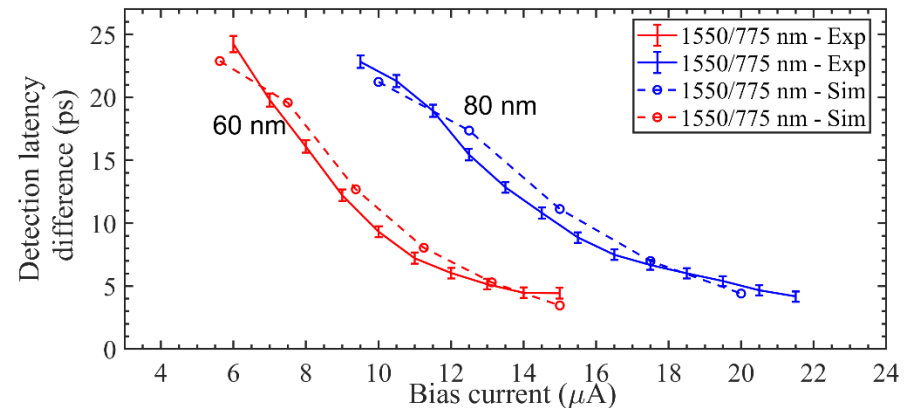
Histogram Comparison



PCR Comparison

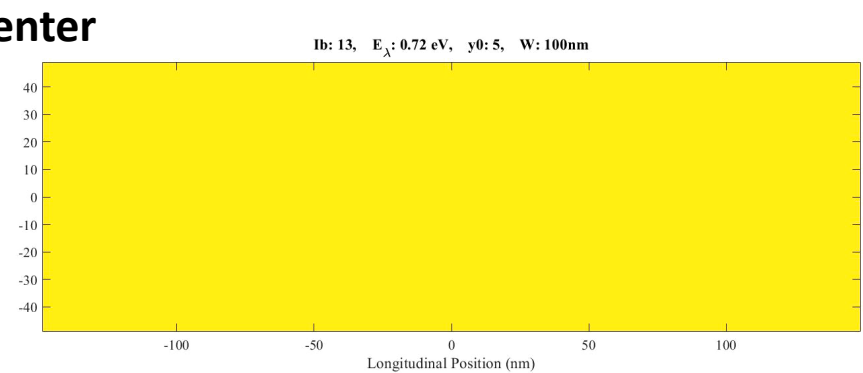
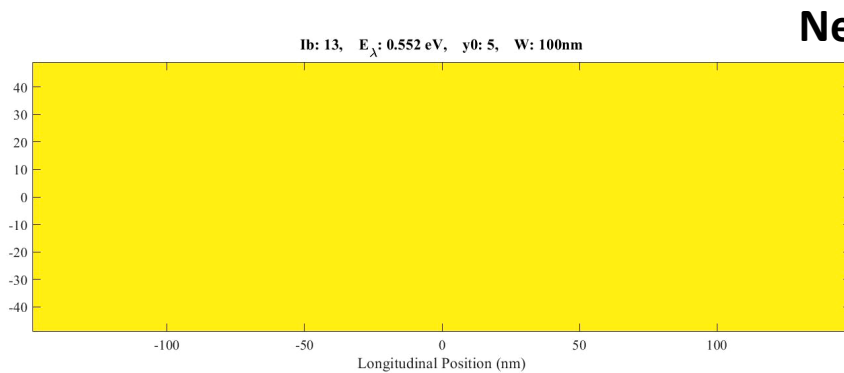


Latency Comparison

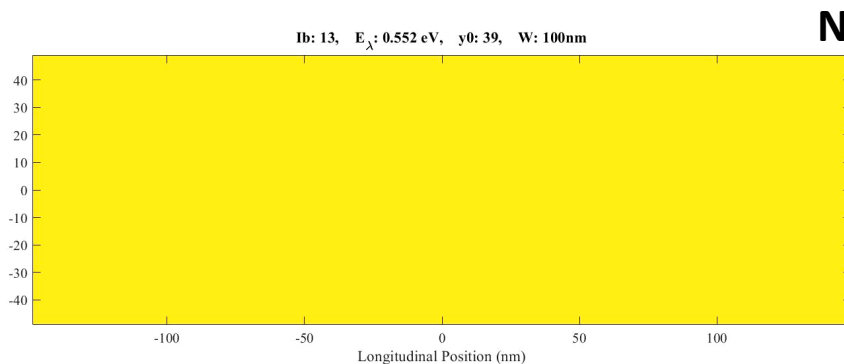


2-Dimensional Model

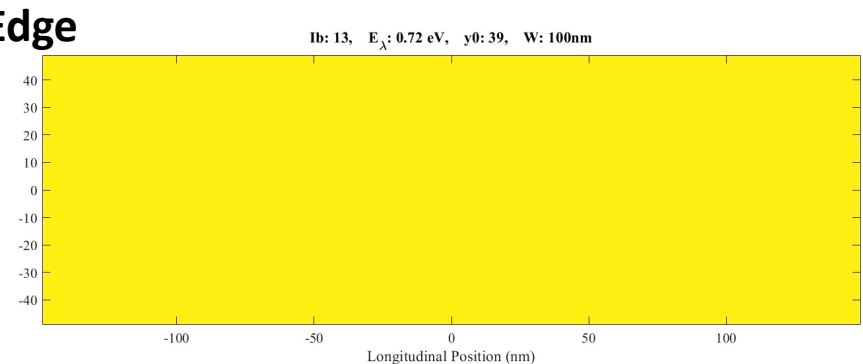
- Vortex formation and motion



Lower Energy – Slower Detection

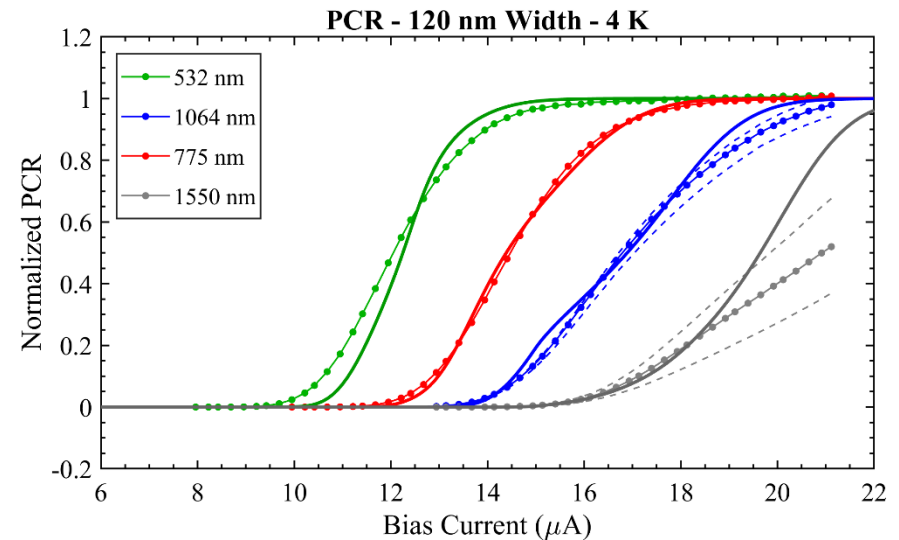
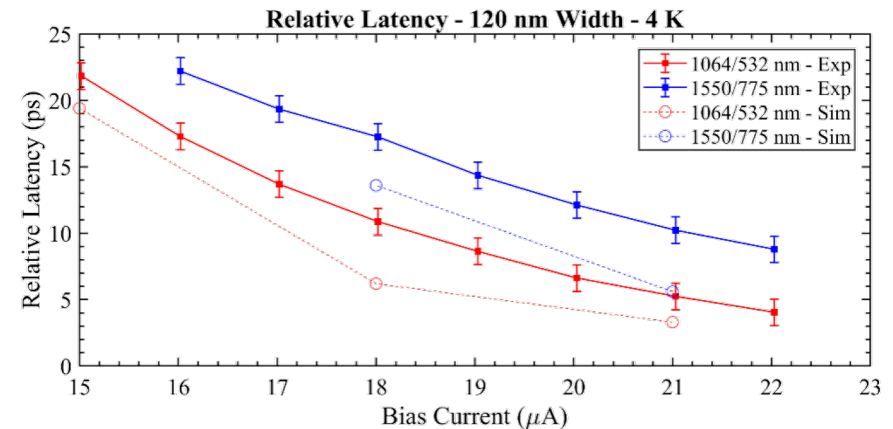


Higher Energy – Faster Detection



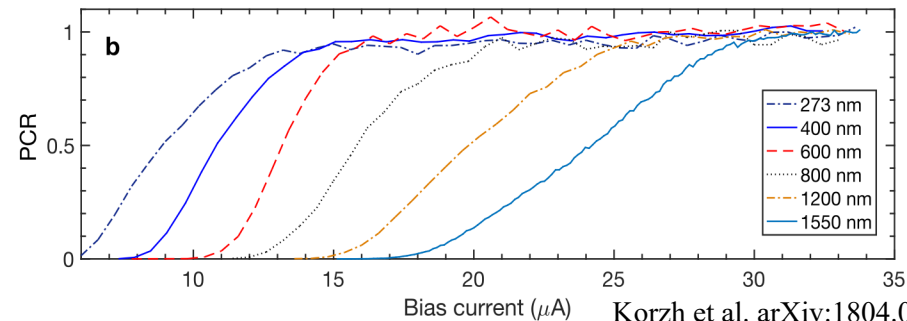
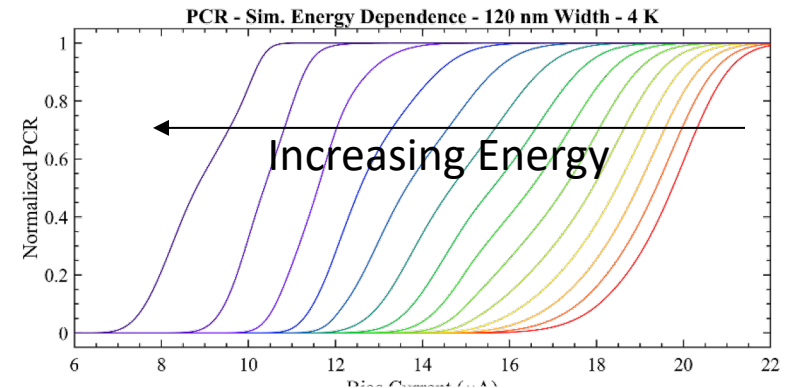
120 nm Wide Device: Model Results

- Generalized TDGL predicts correct latency order of magnitude
- Inadequate match to experimental *PCR*
 - Additional structure appears in simulation due to 2D effects

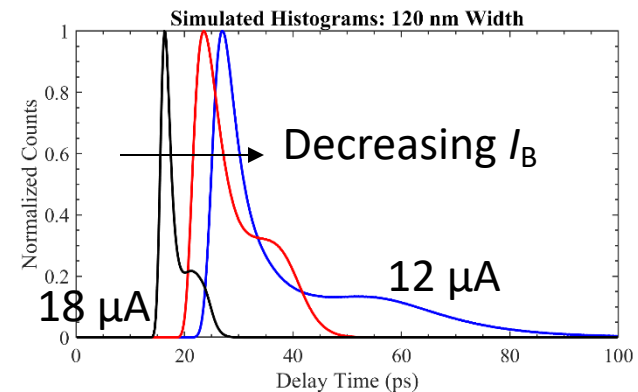
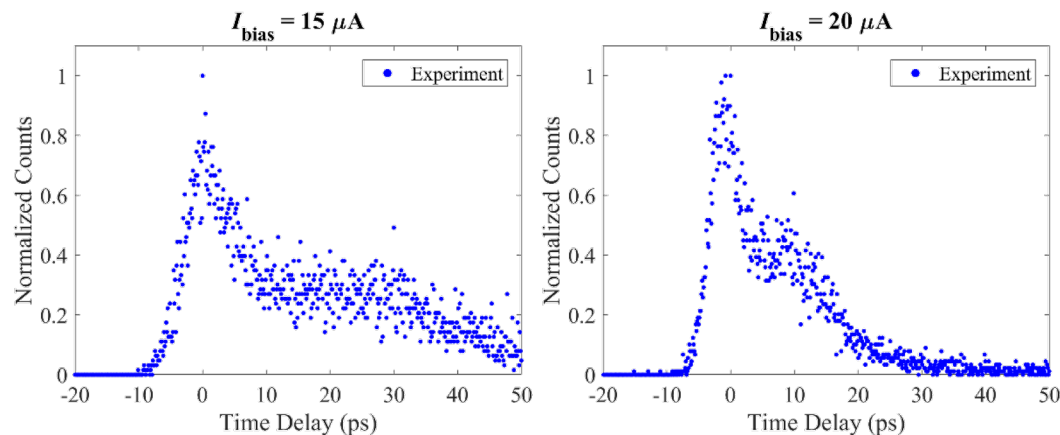


120 nm Wide Device: Model Results

- Correct qualitative trend of PCR curves:
 - Narrowing transition for increased energy,
 - Broadening for extremely high energy (UV)
- Predicts 'shoulder' in high energy jitter histogram for low I_B



Korzh et al. arXiv:1804.06839



Concluding Remarks

- Experimentally able to measure intrinsic jitter, and relative latency, providing information on the timescale of detection
- Model captures qualitative behavior: PCR trends, jitter histogram shape
- Generalized TDGL matches timescale relative latency, unlike the standard TDGL model
- Successful microscopic model must predict 3 metrics: *PCR*, timing jitter, and relative latency



Karl K. Berggren



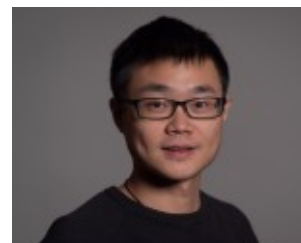
Leonid Levitov



Marco Colangelo



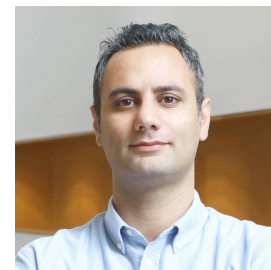
Emily Toomey
NSF Fellowship



Di Zhu
A* STAR Fellowship



Andrew Dane*



Reza Baghdadi
Post-doc



Ilya Charaev
Post-doc

Former Team
Members:
Qingyuen Zhao
Francesco Marsili



Matt Shaw

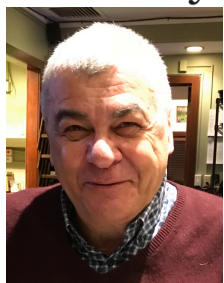


Peter K. Day

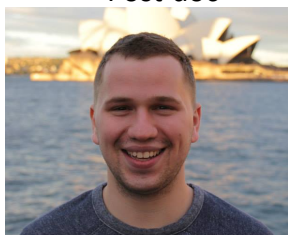


Andrew Beyer

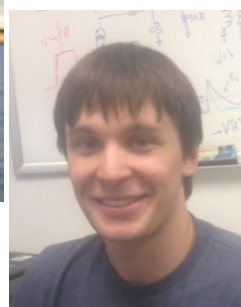
Lancaster
University



Alexander Kozorezov



Eric Bersin*
Edward Ramirez
Garrison Crouch*
*NSTRF/NASA
fellowships



Jason Allmaras*



Simone Frasca



Boris Korzh
Post-doc



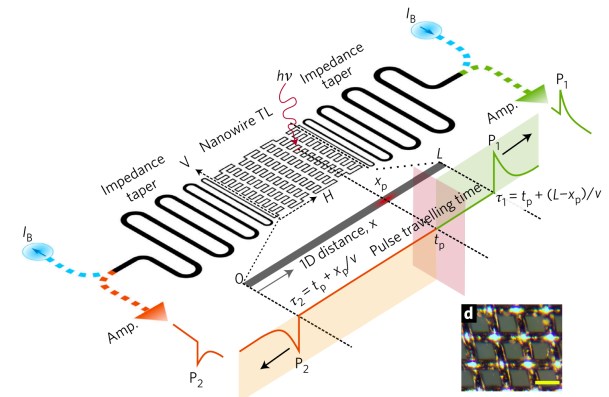
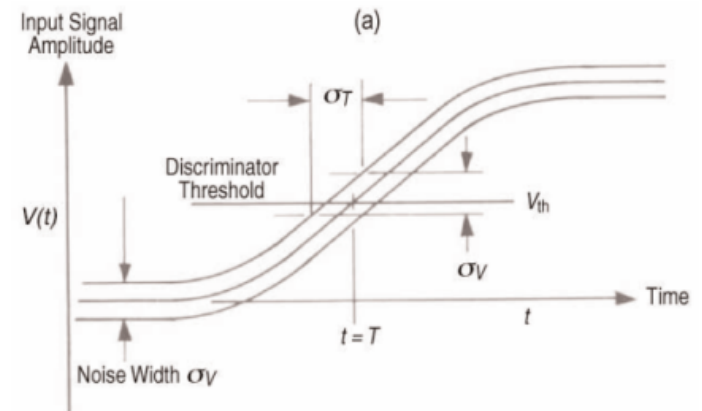
Emma Wollman

Backup Slides

Sources of Timing Jitter

Timing Jitter: Uncertainty in the arrival time of a detected photon

- **Noise Jitter** – electrical noise combined with finite slew rate leads to timing uncertainty
- **Geometric Jitter** – different propagation delays of electrical signal along length of nanowire based on absorption site
- **Inhomogeneity Induced Jitter** – latency changes due to differing nanowire properties at different locations
- **Fano Fluctuations** – latency changes based on the energy retained in the nanowire during detection process
- **Transverse Coordinate Jitter** – latency changes with the absorption site along transverse width of nanowire
- **Additional Fluctuations** – fluctuations during the detection event may influence the time of vortex/phase slip entry

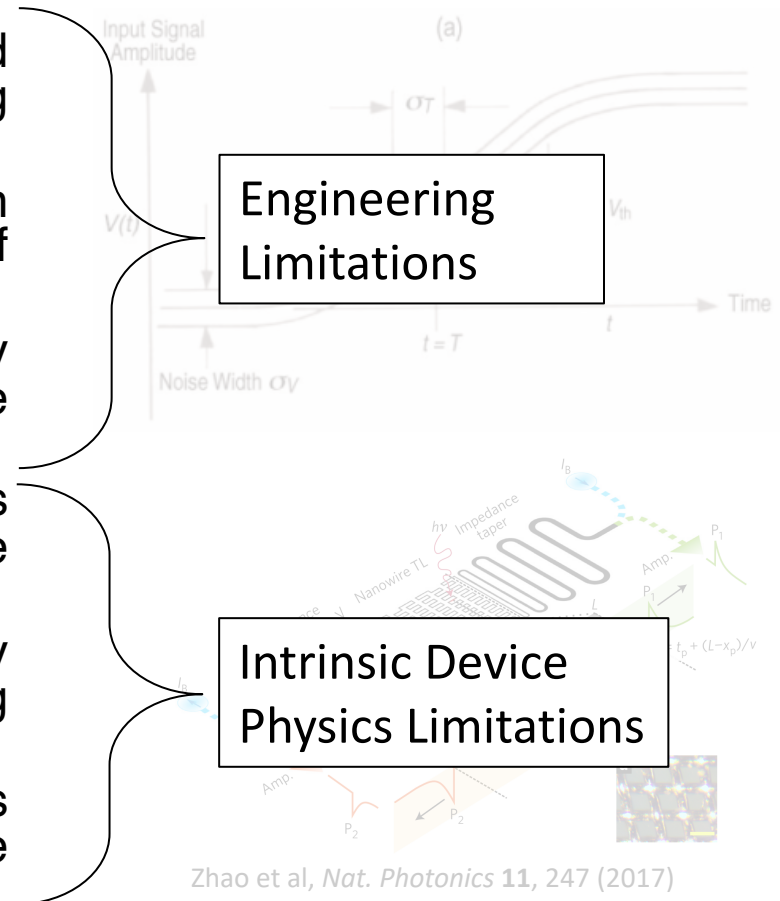


Zhao et al, *Nat. Photonics* **11**, 247 (2017)

Sources of Timing Jitter

Timing Jitter: Uncertainty in the arrival time of a detected photon

- **Noise Jitter** – electrical noise combined with finite slew rate leads to timing uncertainty
- **Geometric Jitter** – different propagation delays of electrical signal along length of nanowire based on absorption site
- **Inhomogeneity Induced Jitter** – latency changes due to differing nanowire properties at different locations
- **Fano Fluctuations** – latency changes based on the energy retained in the nanowire during detection process
- **Transverse Coordinate Jitter** – latency changes with the absorption site along transverse width of nanowire
- **Additional Fluctuations** – fluctuations during the detection event may influence the time of vortex/phase slip entry

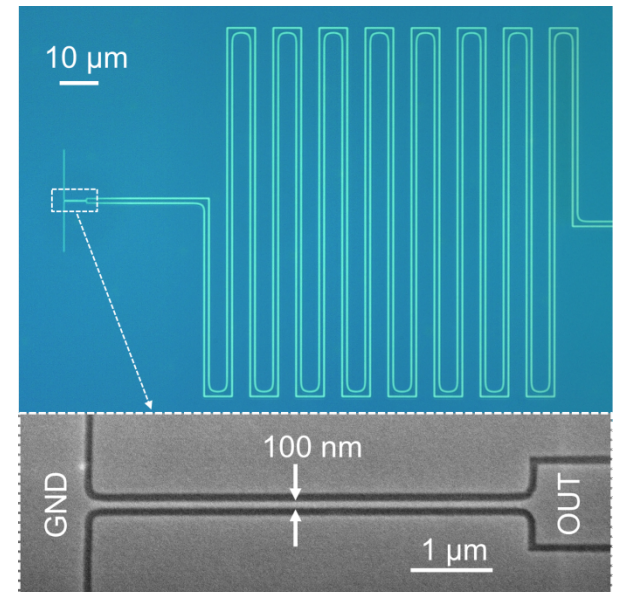


Experimental Approach

- Cosmic Microwave Technology CITLF1 & CITLF3
 - Noise temperature: < 6 K
 - Gain: ~ 40 dB
 - 4 K operation
- $5\text{ }\mu\text{m}$ nanowire length
 - Geometric jitter < 1 ps
- Free space coupling to eliminate dispersion in fiber which broadens optical pulse

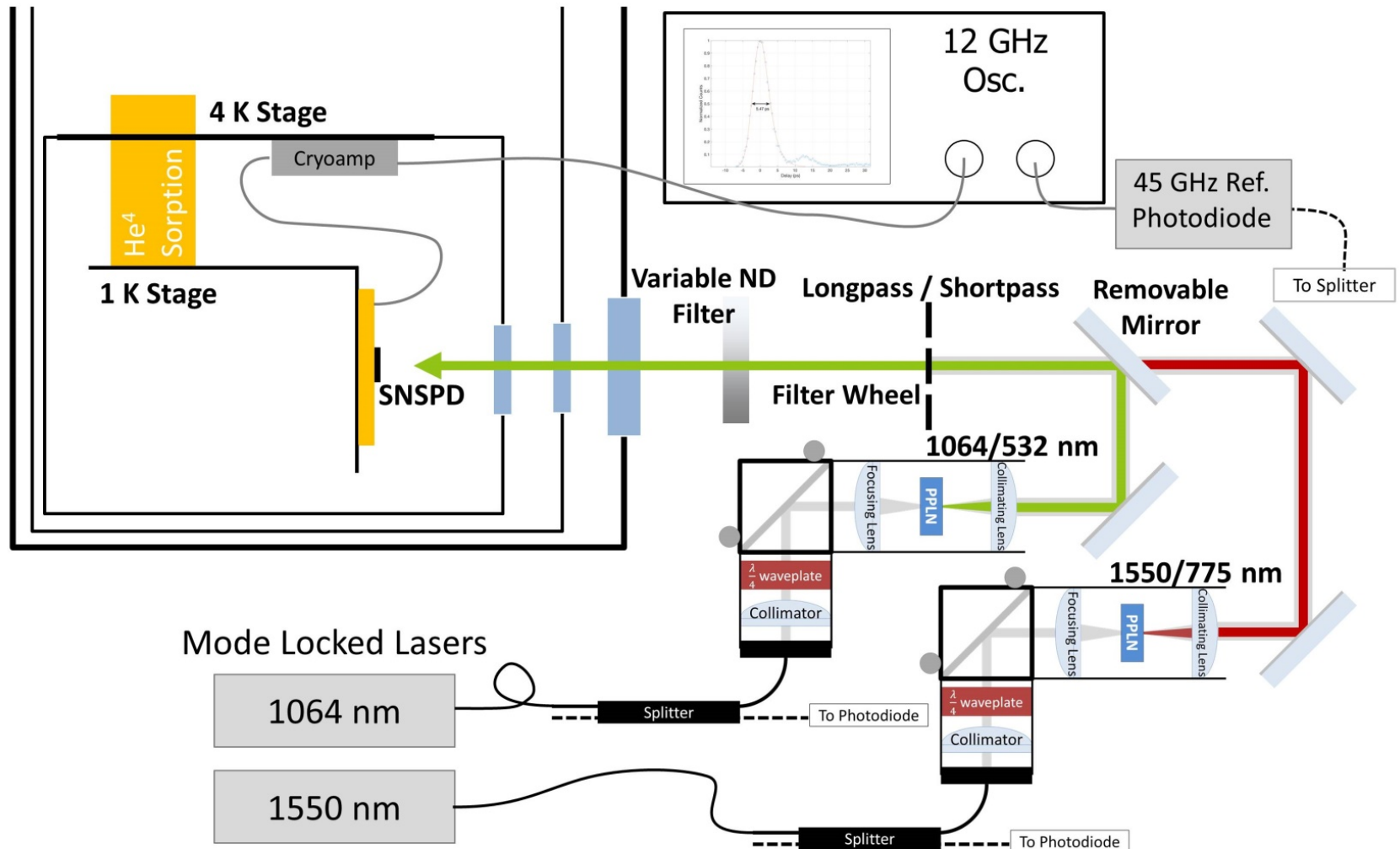


CITLF1



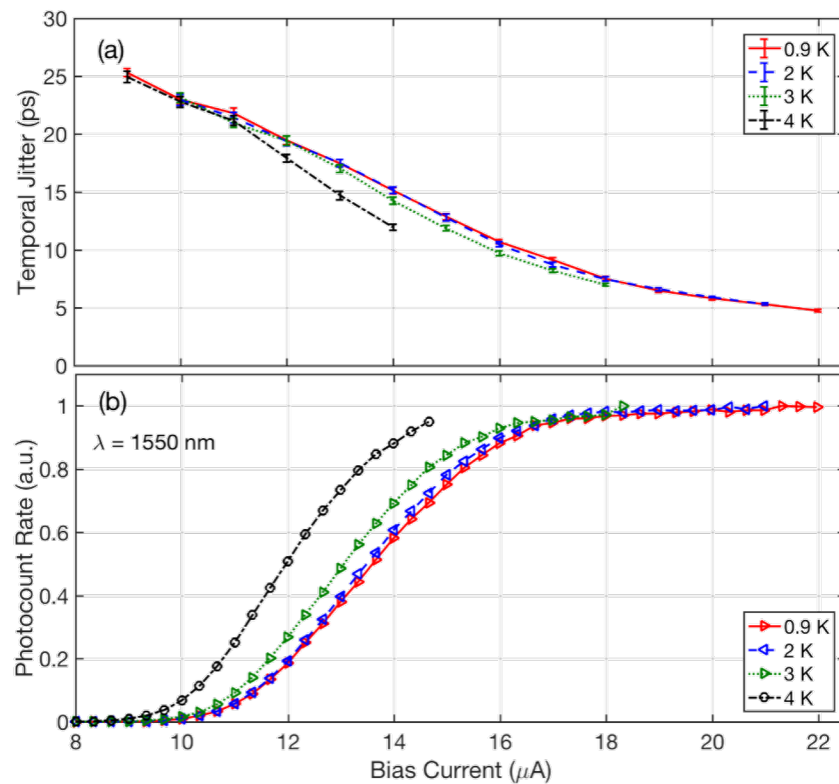
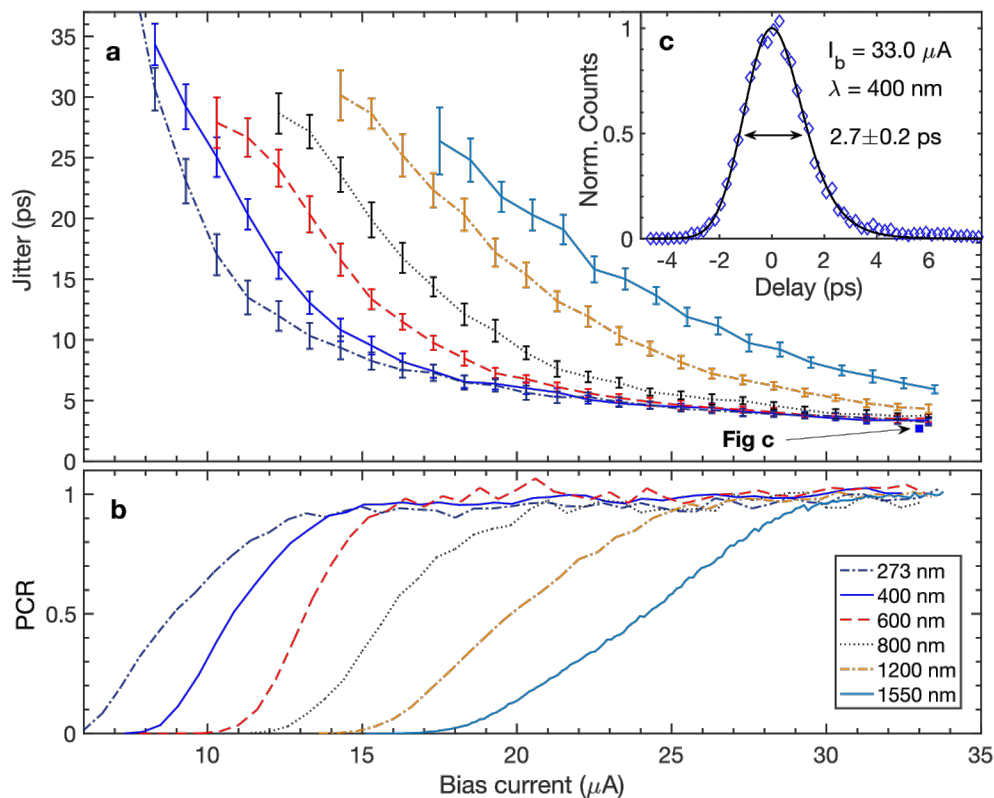
Experimental Setup

- Doubling crystals allow measurement of relative delay between two photon energies



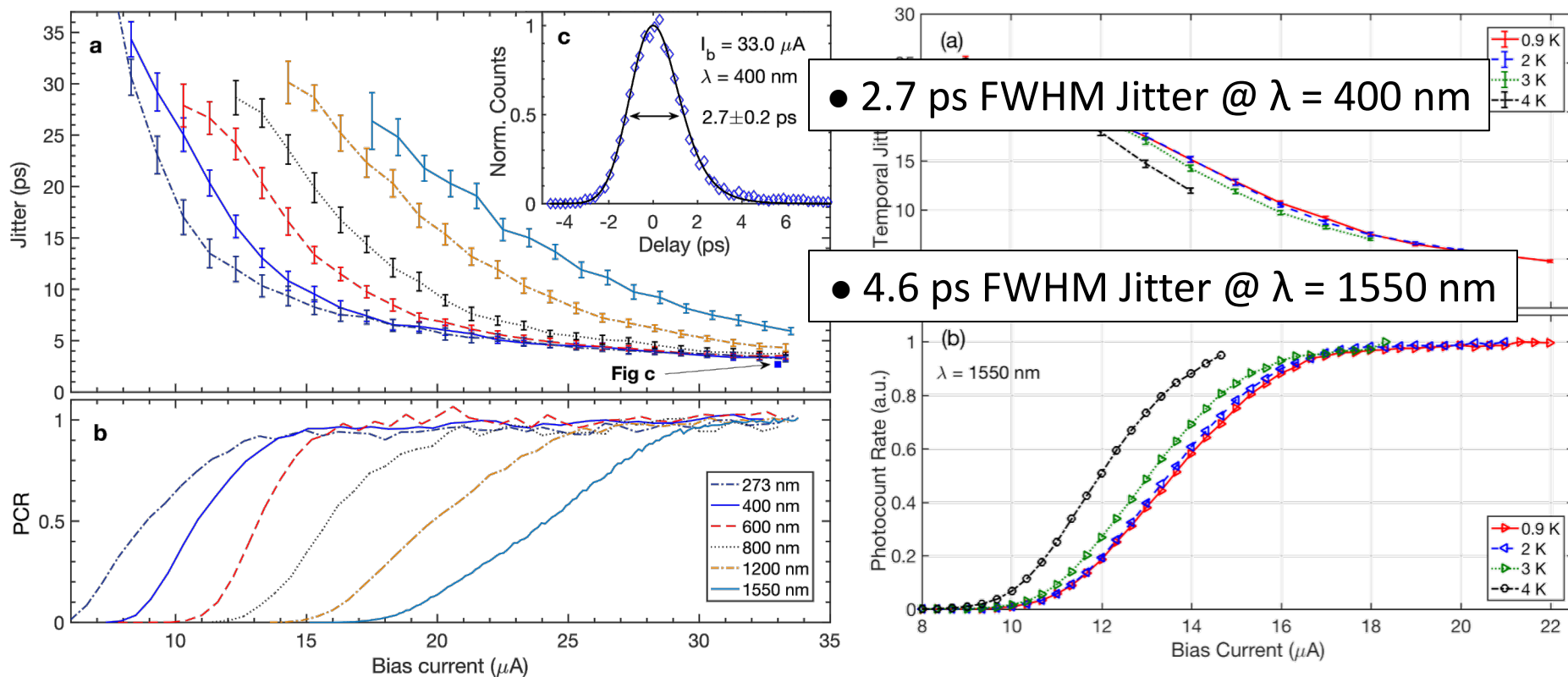
Results: Intrinsic Jitter

- Energy and operating temperature dependence of jitter suggests effects intrinsic to the detection process dominate the jitter



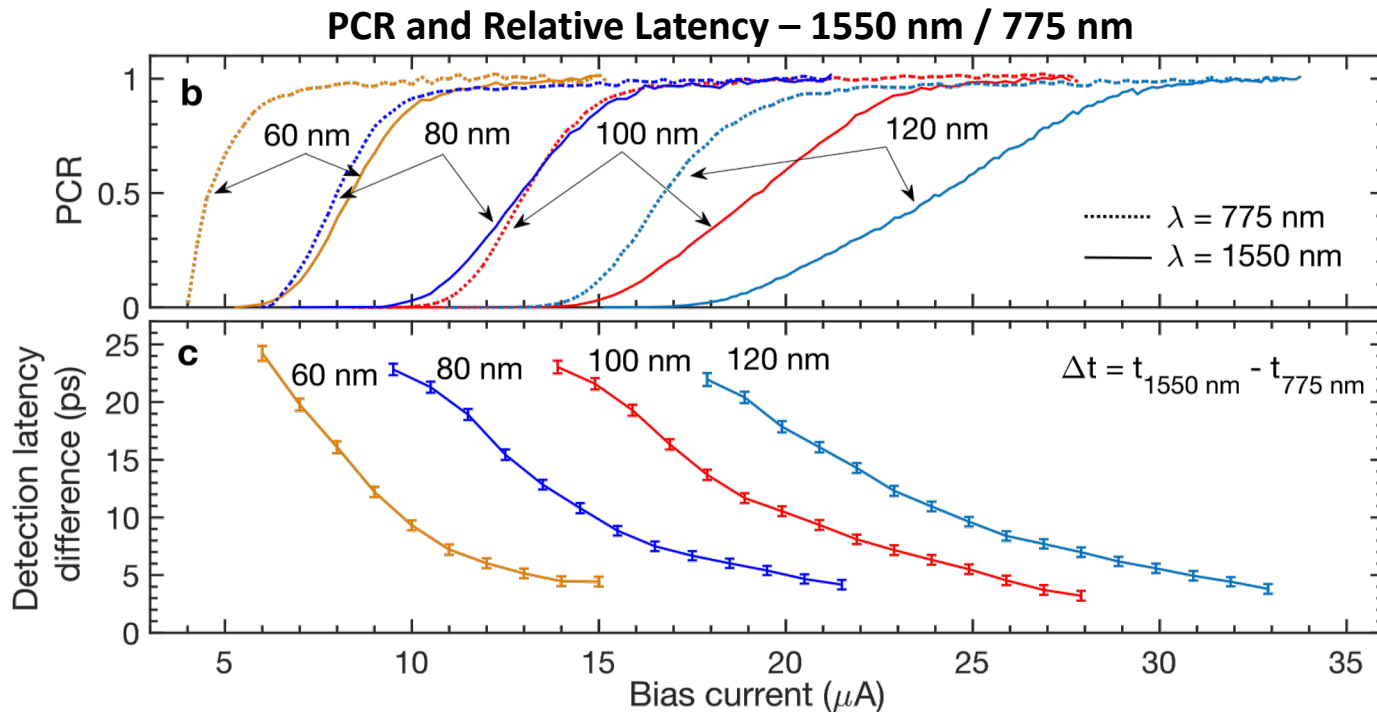
Results: Intrinsic Jitter

- Energy and operating temperature dependence of jitter suggests effects intrinsic to the detection process dominate the jitter



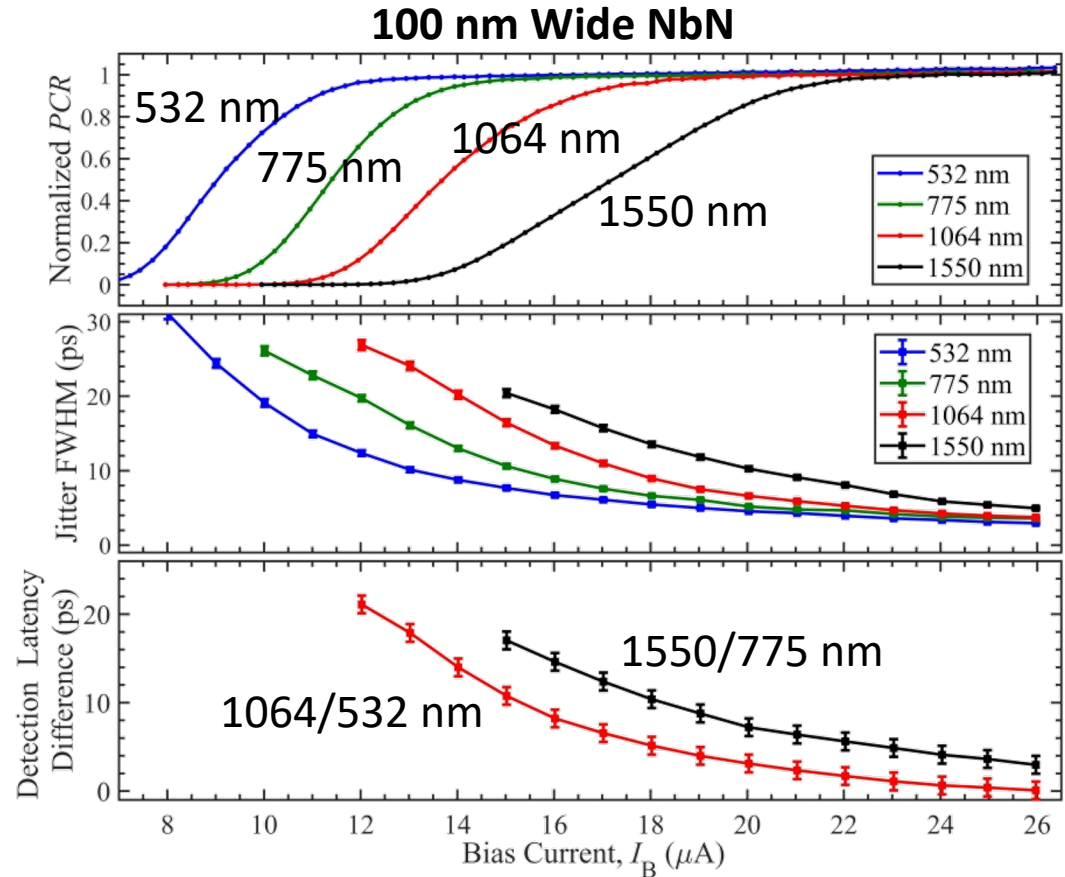
Results: Relative Latency

- Relative latency measured for 1550/775 nm energies for 60 to 120 nm widths
 - Range of relative latency is independent of width

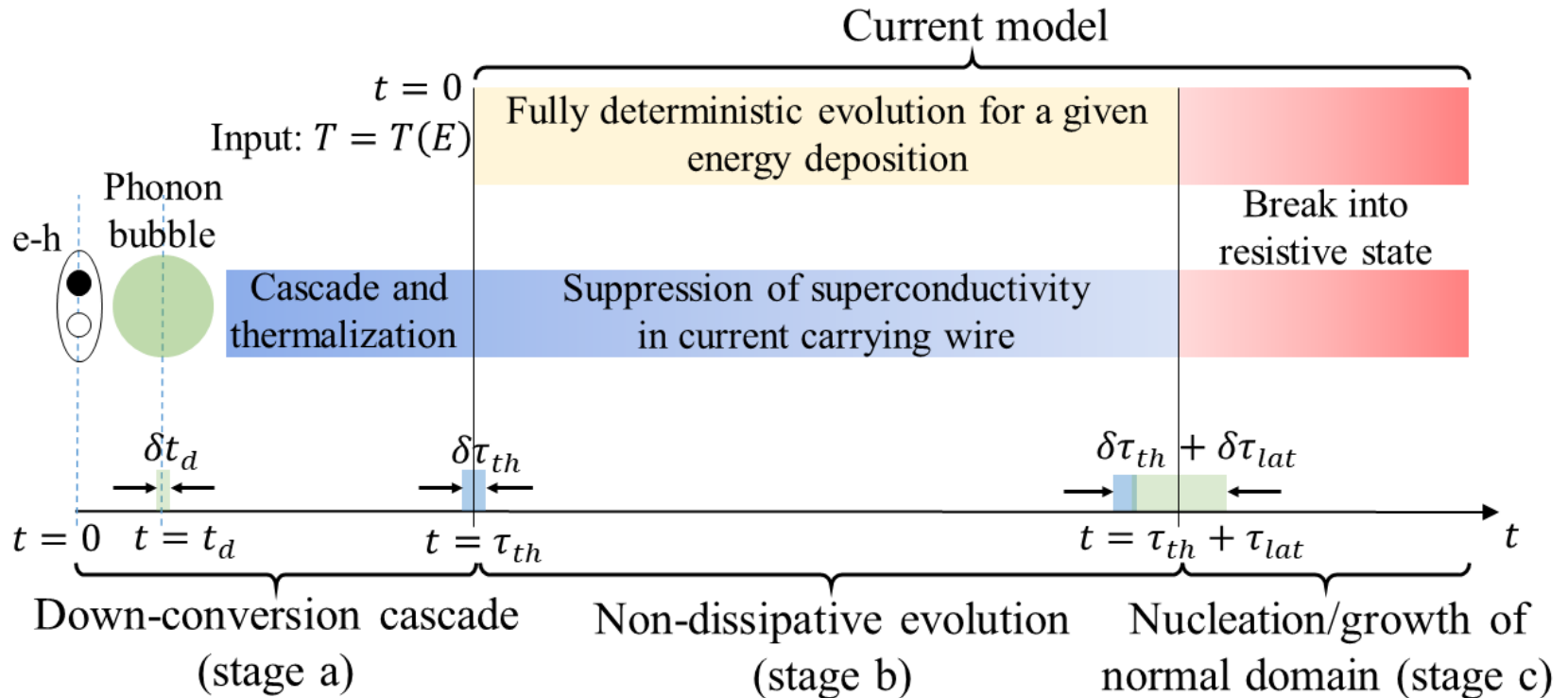


Results: Relative Latency

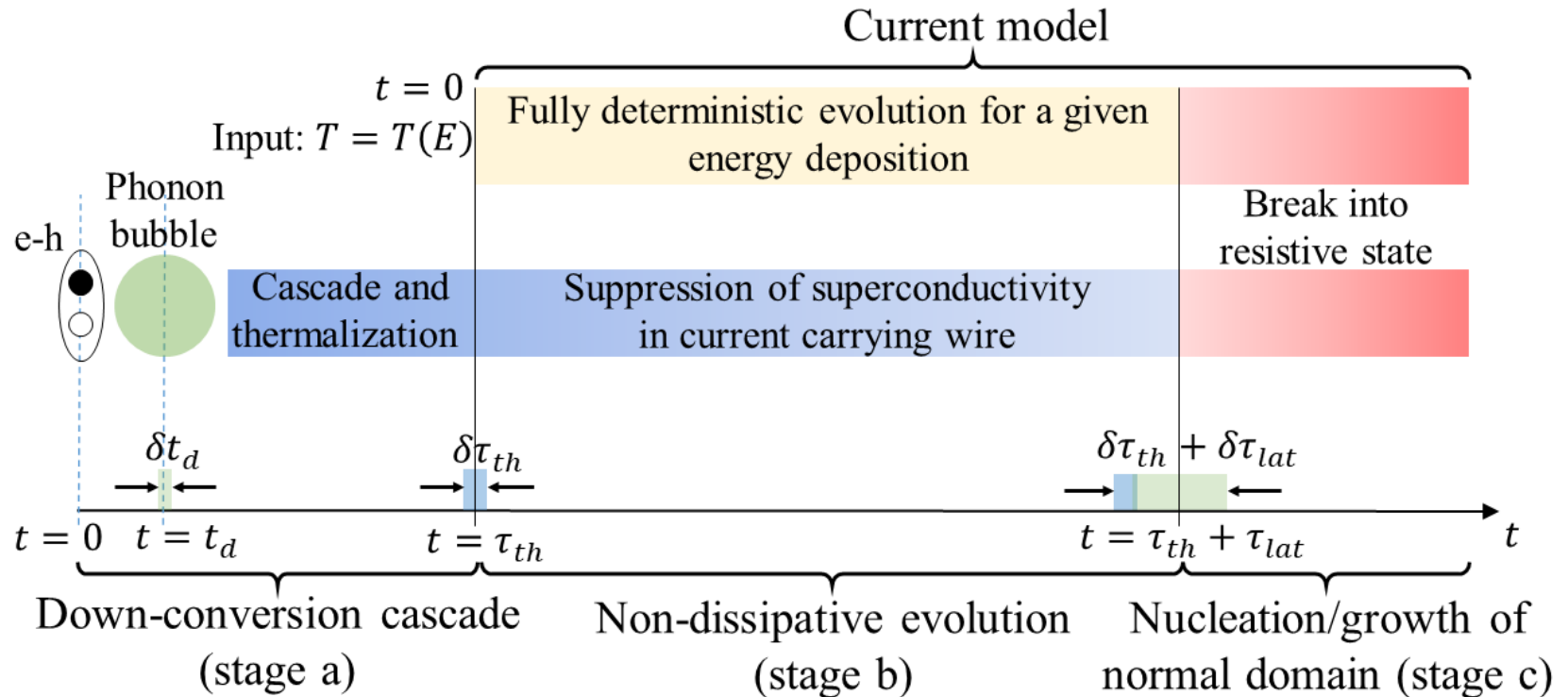
- Addition of 1064/532 nm pair shows a shorter latency difference compared to 1550/775
- Qualitative connection between PCR, jitter, and latency shapes



Model: Stages of Detection



Model: Stages of Detection



- Simplifying Assumptions:
 - All fluctuations occur during downconversion (Fano fluctuations) resulting in different amounts of energy deposited in the superconductor
 - Ignores cascade/thermalization jitter
 - Ignores fluctuations during suppression of superconductivity
 - Ignores inhomogeneity in the nanowire